

AD-A252 146



# NAVAL POSTGRADUATE SCHOOL

## Monterey, California



DTIC  
ELECTE  
JUN 29 1992  
S. D

## THESIS

**SENSITIVITY OF THE TOMOGRAPHIC INVERSE  
SOLUTION TO ACOUSTIC PATH VARIABILITY**

by

**Gary E. English**

**March, 1992**

**Thesis Advisor:**

**Ching-Sang Chiu**

**Approved for public release; distribution is unlimited**

**92-16884**



92 6 9

014

REPORT DOCUMENTATION PAGE				
1a. REPORT SECURITY CLASSIFICATION UNCLASSIFIED		1b. RESTRICTIVE MARKINGS		
2a. SECURITY CLASSIFICATION AUTHORITY		3. DISTRIBUTION/AVAILABILITY OF REPORT Approved for public release; distribution is unlimited.		
2b. DECLASSIFICATION/DOWNGRADING SCHEDULE				
4. PERFORMING ORGANIZATION REPORT NUMBER(S)		5. MONITORING ORGANIZATION REPORT NUMBER(S)		
6a. NAME OF PERFORMING ORGANIZATION Naval Postgraduate School	6b. OFFICE SYMBOL (If applicable) 3A	7a. NAME OF MONITORING ORGANIZATION Naval Postgraduate School		
6c. ADDRESS (City, State, and ZIP Code) Monterey, CA 93943-5000		7b. ADDRESS (City, State, and ZIP Code) Monterey, CA 93943-5000		
8a. NAME OF FUNDING/SPONSORING ORGANIZATION	8b. OFFICE SYMBOL (If applicable)	9. PROCUREMENT INSTRUMENT IDENTIFICATION NUMBER		
8c. ADDRESS (City, State, and ZIP Code)		10. SOURCE OF FUNDING NUMBERS		
		Program Element No.	Project No.	Task No.
				Work Unit Accession Number
11. TITLE (Include Security Classification) Sensitivity of the Tomographic Inverse Solution to Acoustic Path Variability				
12. PERSONAL AUTHOR(S) Gary E. English				
13a. TYPE OF REPORT Master's Thesis	13b. TIME COVERED From To	14. DATE OF REPORT (year, month, day) 1992, March	15. PAGE COUNT 40	
16. SUPPLEMENTARY NOTATION The views expressed in this thesis are those of the author and do not reflect the official policy or position of the Department of Defense or the U.S. Government.				
17. COSATI CODES		18. SUBJECT TERMS (continue on reverse if necessary and identify by block number)		
FIELD	GROUP	SUBGROUP		
		Acoustic Tomograph, Multipath Variability		
19. ABSTRACT (continue on reverse if necessary and identify by block number)				
<p>As part of the Greenland Sea Project Woods Hole Oceanographic Institution and Scripps Institute of Oceanography deployed six acoustic tomography transceiver moorings to measure variability of the Greenland Sea gyre through a cooling cycle from September 1988 to August 1989. Using a set of Greenland Sea acoustic tomography data provided by Woods Hole Oceanographic Institution this thesis investigated the importance of incorporating acoustic path changes in the construction of the tomographic inverse solution.</p> <p>A comparison of the inverse solutions for changes in sound speed using non-corrected and corrected acoustic multipaths was conducted. Although the two inverse solutions are qualitatively similar, significant quantitative differences exist. These differences indicate that it is necessary to account for changes in the acoustic multipaths for the generation of accurate Greenland Sea acoustic tomography maps.</p>				
20. DISTRIBUTION/AVAILABILITY OF ABSTRACT <input checked="" type="checkbox"/> UNCLASSIFIED/UNLIMITED <input type="checkbox"/> SAME AS REPORT <input type="checkbox"/> DTIC USERS		21. ABSTRACT SECURITY CLASSIFICATION UNCLASSIFIED		
22a. NAME OF RESPONSIBLE INDIVIDUAL Ching-Sang Chiu		22b. TELEPHONE (Include Area code) (408) 646-3239		22c. OFFICE SYMBOL Code OC/CI

Approved for public release; distribution is unlimited.

**Sensitivity of the Tomographic Inverse  
Solution to Acoustic Path Variability**

by

**Gary E. English**  
Lieutenant, United States Navy  
B.S., United States Navy Academy, 1984

Submitted in partial fulfillment  
of the requirements for the degree of

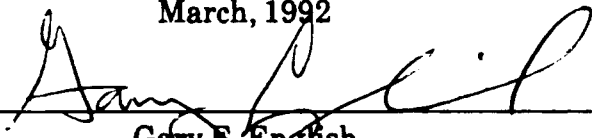
**MASTER OF SCIENCE IN APPLIED SCIENCE  
(ANTI-SUBMARINE WARFARE)**

from the

**NAVAL POSTGRADUATE SCHOOL**

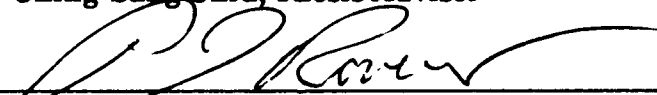
March, 1992

Author:

  
\_\_\_\_\_  
Gary E. English

Approved by:

  
\_\_\_\_\_  
Ching-Sang Chiu, Thesis Advisor

  
\_\_\_\_\_  
LCDR Peter J. Rovero, USN, Second Reader

  
\_\_\_\_\_  
James N. Eagle, Chairman  
Anti-Submarine Warfare Academic Group

# ABSTRACT

As part of the Greenland Sea Project Woods Hole Oceanographic Institution and Scripps Institute of Oceanography deployed six acoustic tomography transceiver moorings to measure variability of the Greenland Sea gyre through a cooling cycle from September 1988 to August 1989. Using a set of Greenland Sea acoustic tomography data provided by Woods Hole Oceanographic Institution this thesis investigated the importance of incorporating acoustic path changes in the construction of the tomographic inverse solution.

A comparison of the inverse solutions for changes in sound speed using non-corrected and corrected acoustic multipaths was conducted. Although the two inverse solutions are qualitatively similar, significant quantitative differences exist. These differences indicate that it is necessary to account for changes in the acoustic multipaths for the generation of accurate Greenland Sea acoustic tomography.



Accession For	
NTIS GRA&I	<input checked="" type="checkbox"/>
DTIC TAB	<input type="checkbox"/>
Unannounced	<input type="checkbox"/>
Justification	
By	
Distribution/	
Availability Codes	
Dist	Avail and/or Special
A-1	

## TABLE OF CONTENTS

I. INTRODUCTION . . . . .	1
A. OCEAN ACOUSTIC TOMOGRAPHY . . . . .	1
B. GREENLAND SEA PROJECT . . . . .	2
C. OBJECTIVE . . . . .	3
D. APPROACH . . . . .	3
II. DESCRIPTION OF APPROACH . . . . .	8
A. INTERFACE MPP TO INVERSION CODE . . . . .	8
B. ESTIMATING ABSOLUTE POSITION ERROR . . . . .	10
C. TRAVEL TIME TIME SERIES . . . . .	11
D. STATIC RAY APPROXIMATION . . . . .	11
E. UPDATED RAY GEOMETRY . . . . .	12
III. INVERSION RESULTS AND DISCUSSION . . . . .	14
A. ABSOLUTE POSITION ERROR . . . . .	14
B. INVERSION USING STATIC RAY APPROXIMATION . . . . .	14
C. INVERSION USING UPDATED RAY GEOMETRY . . . . .	20
IV. CONCLUSIONS AND RECOMMENDATIONS . . . . .	31
REFERENCES . . . . .	32

INITIAL DISTRIBUTION LIST . . . . .	33
-------------------------------------	----

## I. INTRODUCTION

### A. OCEAN ACOUSTIC TOMOGRAPHY

The purpose of tomography is to remotely sense the interior structure of a desired medium. This may be done through a variety of methods. X-rays are used in medical computer assisted tomography (CAT) scans and seismic waves are introduced by surface sources in the study of the interior structure of the earth. Ocean acoustic tomography is accomplished by transmitting sound waves through the sea, a medium which is relatively transparent to sound.

Munk and Wunsch (1979) first introduced the procedure of using acoustic inverse techniques to monitor ocean basins for mesoscale fluctuations. The application of acoustic tomography to monitor the interior structure of the ocean has two parts. The first part of acoustic tomography is to solve the "forward" problem. Sound propagates through the ocean from a source to a receiver along the acoustic multipaths. Measured travel time changes of the sound signals along these paths constitute the data of this underwater acoustic observing system. Given a reference sound speed field, it is necessary to predict the geometry and travel time of sound waves along these acoustic multipaths. This can be done by using ray tracing computer programs. The second part of

acoustic tomography is solving the "inverse" problem. Travel time changes of sound signals are used to infer changes in the sound speed field. The inversion of travel time changes can be accomplished by a linear, minimum mean square error estimator as has been shown by Cornuelle et al. (1985), Chiu et al. (1987), and Joseph (1991).

#### **B. GREENLAND SEA PROJECT**

The Greenland Sea Project (GSP) is a five year (1987-1992), international scientific study to understand the large scale, long term interactions of air, sea, and ice in the Greenland Sea. The five key elements of GSP are to study the air-sea-ice interaction, ocean ventilation, ocean circulation and mixing, atmospheric energetics, and biological processes.

As part of GSP, an array of six tomography transceivers were deployed in the Greenland Sea in the fall of 1988, by Woods Hole Oceanographic Institution (WHOI) and Scripps Institute of Oceanography (SIO). The role of ocean acoustic tomography was to assist in the studies of ocean ventilation and circulation. The array of transceiver moorings is designed to measure changes in the integrated properties of the Greenland Sea gyre through a winter cooling season (Greenland Sea Science Planning Group, 1986). Figure 1 shows the deployment site and geometry of the array. Each mooring transmitted an acoustic signal six times a day every third day, during the period of September 1988-August 1989. Table



1 provides the transceiver locations. The latitude and longitude of the moorings were converted to an XY plane by Joseph (1991). This operation was conducted by placing a 240 km by 240 km grid over the six transceivers. The grid was centered on Mooring 6. Figure 2 depicts the grid system used to convert the mooring position to XY coordinates.

### **C. OBJECTIVE**

The objective of this thesis is to investigate the importance of incorporating acoustic path variability in the tomographic inverse solution. Travel time of sound signal along an acoustic path is affected by changes in the sound speed along the path. In addition, it is also affected by changes in the path. In the construction of the inverse solution, the path is usually held stationary and only the changes in sound speed are considered. It is the intent of this study to determine if path geometry changes need to be considered in the inversion of the Greenland Sea tomography data.

### **D. APPROACH**

The thesis objective was met by comparison of the inverse solutions for changes in sound speed obtained using non-corrected and corrected multipaths. Only the transmissions between Moorings 4 and 5 were used in my investigation. The acoustic travel time data were provided by WHOI. The

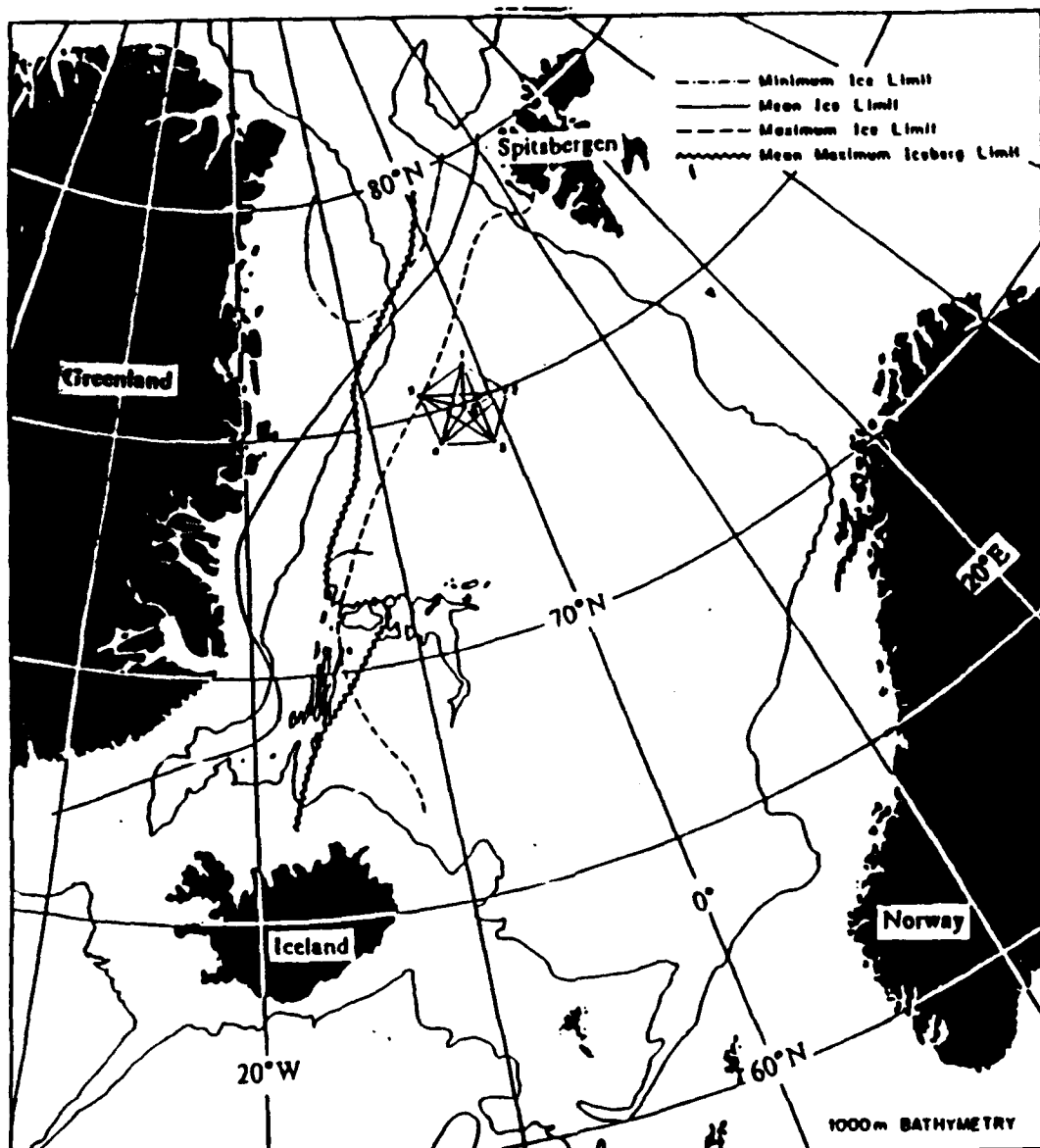


Figure 1. Deployment Site of the Greenland Sea Tomography Array. (from Greenland Sea Science Planning Group, 1986)

**Table I: TRANSCEIVER LOCATIONS.** (from Joseph, 1991)

Mooring	Lat-Long Position	X-Y Position (km)	Source Depth(m)	Receiver Depth(m)
1	75°58.08'N,001°50.00'W	154.790 220.317	99.7	150.4
2	75°03.69'N,000°40.25'E	224.683 119.080	94.0	150.4
2a	75°03.88'N,000°38.20'E	223.715 119.491	97.4	148.1
3	74°09.38'N,001°52.90'W	148.972 18.146	96.0	146.7
4	74°28.90'N,005°47.30'W	33.270 60.958	94.6	117.7
5	75°34.27'N,006°07.70'W	34.547 182.902	101.5	124.6
6	75°03.60'N,002°58.00'W	120.000 120.000	92.5	143.2

"forward" problem was solved by using the Multiple-Profile Ray Tracing Program (MPP), a ray theory based algorithm, to calculate the acoustic multipaths. MPP was developed by Spofford (1973). The output from MPP was then interfaced with the inversion code to calculate the estimated change in sound speed ( $\delta c$ ). The inversion code was developed by Chiu (1987) and modified by Joseph (1991).

All the inversions performed in this thesis used a twelve day average of the observed data. That is, twelve-day-averaged travel time changes were used as input to the inversion code. The first method of data inversion used non-corrected multipaths. The non-corrected multipaths were calculated by MPP using a range independent Sound Velocity Profile (SVP). This SVP was measured by WHOI and SIO during

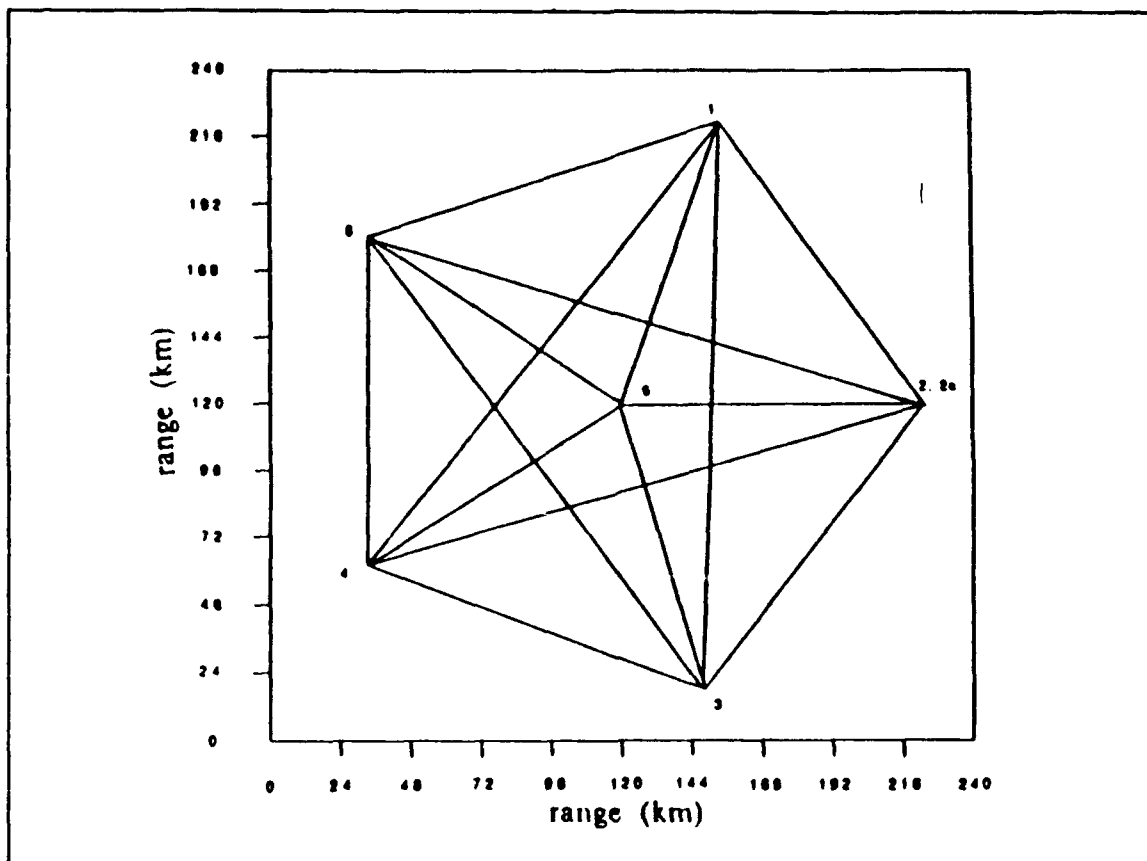


Figure 2. PLAN VIEW OF ARRAY GEOMETRY. (from Joseph, 1991)

the deployment of the moorings. The multipaths were held constant through a period from day 270 to day 342. The study will focus on this period. This procedure will be referred to as the static ray approximation. The second method of data inversion used corrected (i.e., updated) multipaths. The initial multipaths were exactly the same as those used in the static ray approximation. However, as time progressed, the background profiles were updated. This created a set of range dependent SVPs for MPP to calculate updated multipaths. This procedure will be referred to as the updated ray geometry. If the  $\delta c$  maps generated by the two methods show significant

differences, then it would be necessary to account for changes in the acoustic multipaths in the inversions of the Greenland Sea tomography data.

## II. DESCRIPTION OF APPROACH

This chapter details the systematic approach used to achieve the thesis objective as stated in the introduction. MPP was used to predict the acoustic multipaths or eigenrays. All eigenrays were calculated from a source at Mooring 4 to a receiver at Mooring 5. Only this mooring pair was used in this study. Eigenrays are the paths that acoustic signals travel for a particular source-receiver geometry. In the Greenland Sea, eigenrays are usually grouped in bundles of four. The initial angles of the rays in a bundle are within a few tenths of a degree from each other. Two of the rays in a bundle start in a downward direction and the other two start in an upward direction. Upon arrival at the receiver two rays in the bundle arrive from beneath the receiver and two from above. For our inverse analysis we have used the four rays in the 13 degree bundle, containing three lower turning points, the 10 degree bundle, containing four lower turning points, and the slowest arrival from the zero degree path.

### A. INTERFACE MPP TO INVERSION CODE

MPP was used to calculate eigenrays within an initial angles of  $\pm 20^\circ$ . Eigenrays were traced from the source to the receiver in both range independent and range dependent modes. Multiple SVP profiles at a designated interval of 24 km

between profiles were used in each range dependent run. MPP linearly interpolated at 30 evenly spaced intervals between the designated profiles. For all runs a flat bottom at a depth of 5000 m was assumed. No bottom-interacting eigenrays were used for the subsequent inverse analysis.

MPP's output provides the initial angle (degrees), the number of discretized ray coordinates (integer variable), and travel time (s) of each eigenray. The output also provides at unevenly spaced horizontal range intervals, the ray coordinates (range (km) versus depth (km)), grazing angle (radians), and sound speed (km/s) along each eigenray.

The output data from MPP was rearranged into an acceptable format for the inversion code. The rearrangement used cubic splines to interpolate the ray coordinates from a variable number of unevenly spaced horizontal range intervals into 500 evenly spaced intervals.

The inversion code was set up by Joseph (1991) to map sound speed perturbation  $\delta c(x,y,z)$  in a 240 km x 240 km x 3 km ocean volume centered on Mooring 6. The horizontal dimensions were divided into ten 24 km segments. The vertical dimension was divided into five layers of variable thickness. The layers were centered at 100 m, 200 m, 450 m, 750 m, and 1500 m depths, respectively. These divisions and layering discretized the ocean volume into 500 three dimensional boxes. It is essential for the estimator to accurately determine the

amount of path length a ray has in each box based on the input ray coordinates.

To incorporate path dynamics in the inversions of the observed travel time changes (12 day averages), the estimated change in sound speed ( $\delta c$ ) calculated at a 12 day time step was used to update the background profiles and hence the ray geometry for the inversion at the next time step. This procedure will be discussed in greater detail later in this chapter.

#### B. ESTIMATING ABSOLUTE POSITION ERROR

It is important to estimate the absolute range error so that the corresponding travel time bias can be removed from the data. To determine the absolute range error between the source and the receiver the differences in the mean travel time of the observed signals and the travel time predicted by MPP for the 13 degree bundle was used. The observed mean travel times ( $\bar{T}_o$ ) were obtained by averaging the data over a period of 11 months. The predicted travel times ( $T_c$ ) were calculated using the background profile shown in Figure 3, in a range independent mode.

To correct the horizontal range between the source and receiver, the following relation was used

$$\delta x = \bar{c}(T_o - T_c) \quad (1)$$



where  $\delta x$  is the horizontal range error and  $\bar{c}$  is a mean sound speed. Multiple MPP runs were made varying  $\delta x$  until the calculated and observed travel times matched each other for the 13 degree bundle.

### **C. TRAVEL TIME TIME SERIES**

The data file provided by WHOI was used to construct a travel time time series for this study. Each transmission day consisted of six transmissions. These gave six travel times for each individual eigenray. The travel times were corrected for relative mooring motion and averaged over each transmission day. They were then averaged over twelve day intervals. The last day of each interval was used as the first day of the next twelve day period. These twelve day travel time averages were used for both the static ray approximation and updated ray geometry inversions.

Throughout the remainder of this thesis, day XXX, such as day 270, will be used to denote a twelve day period centered at that day.

### **D. STATIC RAY APPROXIMATION**

There are two primary ways in which the travel time of sound signals are affected. The first is by fluctuations in the sound speed and the second is by fluctuations in the ray paths. The neglect of the second effect in the inversions of data over the period of the experiment constitutes the static

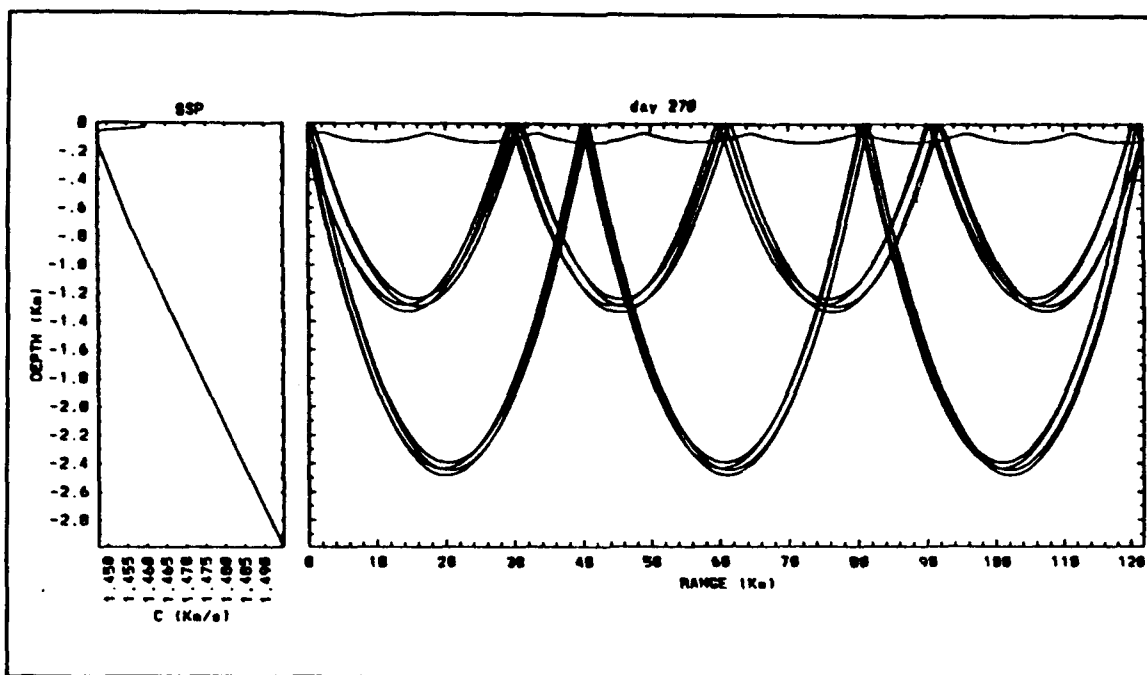


**Figure 3. BACKGROUND SVP AND CALCULATED EIGENRAYS USED IN THE STATIC RAY APPROXIMATION INVERSION.**

ray approximation.

Nine eigenrays were calculated by MPP using the range independent background profile shown in Figure 3. The calculated eigenrays are also presented in this figure. The rays were held constant for each of the inversions over the period considered.

#### **E. UPDATED RAY GEOMETRY**

To account for the fluctuations in ray paths over the experimental period, I updated the eigenrays after the inversion of the data at each time step in the time series.

The initial inversion at day 270 utilized the same range independent profile and eigenray geometry as displayed in

Figure 3. An estimated  $\delta c$  map was generated by the inversion code. This map was used to update the range independent background profile. A series of range dependent SVPs resulted from these corrections. Updated ray paths were then calculated by MPP using the range dependent profiles, and were used for the next inversion. In updating the background and ray geometry,  $\delta c$  was linearly interpolated between boxes and eigenrays were retraced. This process was repeated for each inversion in the time series.

### **III. INVERSION RESULTS AND DISCUSSION**

#### **A. ABSOLUTE POSITION ERROR**

The 13 degree ray bundle was used for the range correction. This bundle spent the least amount of time in the near surface layer which contained the greatest variability and thus would be least susceptible to its effects. Table III shows that the travel times calculated by MPP based on the range given by Joseph (1991) were on the average 219 ms faster than the observed travel times. An initial estimate of 320 m for the error in horizontal range was calculated. Several MPP runs were conducted in which the position of the source was fixed and the horizontal range to the receiver was increased until the optimal range correction was obtained. The final results listed in Table III demonstrate that with a correction of +322 m MPP was able to calculate travel times of the 13 degree bundle to within an average of 1.98 ms of the observed mean travel time. The addition of this +322 m to the horizontal range would ensure that the differences between the observed and calculated travel time was due mainly to ocean variability.

#### **B. INVERSION USING STATIC RAY APPROXIMATION**

Inversions using the static ray approximation were conducted using the procedures previously outlined. Figure 3

**Table II: TRAVEL TIME BIAS AND CORRECTION**

104 DAY AVERAGED TRAVEL TIMES (s)	MPP CALCULATED TRAVEL TIMES (s)	$\delta T$ (s)	322 m OFFSET TRAVEL TIMES (s)	OFFSET $\delta T$ (s)
13 DEGREE BUNDLE				
83.8541	83.6373	.21688	83.8539	.0002
83.8806	83.6639	.21670	83.8808	-.0002
83.8941	83.6731	.22100	83.8903	.0038
83.9207	83.6997	.22100	83.9166	.0041
10 DEGREE BUNDLE				
84.2107	83.9760	.23470	84.1957	.0150
84.2180	83.9923	.22570	84.2121	.0059
84.2391	83.9988	.24030	84.2187	.0204
84.2454	84.0143	.23110	84.2343	.0111
ZERO DEGREE RAY				
84.5395	84.2402	.29930	84.4633	.0762

contains the range independent background profile used by MPP to calculate the associated eigenrays. Figure 4 is a map of the estimated  $\delta c$  from the inversion for day 270. This map is the same for both inversion procedures considered in this study. This figure demonstrated the greatest amount of variability takes place in the upper 1000 m. The sound speed minimum occurs at approximately 100 m. The source and receiver are located within the vicinity of the sound speed minimum.

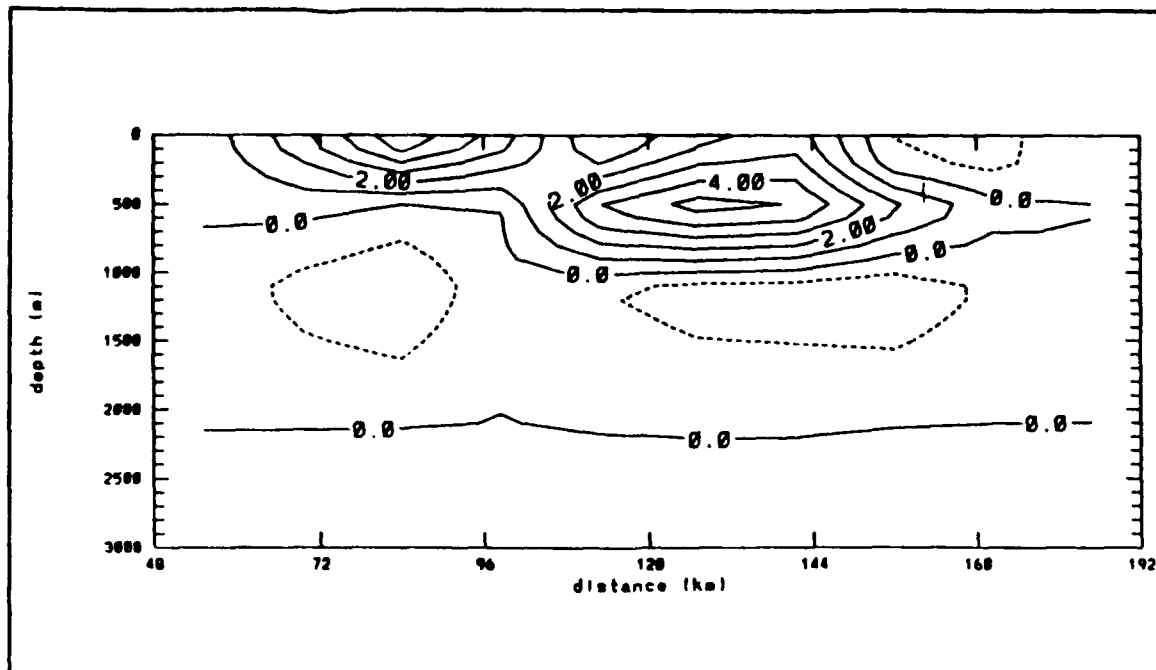


Figure 4. ESTIMATED  $\delta c$  FOR DAY 270 USING THE STATIC RAY APPROXIMATION. (contour interval is 1 m/s)

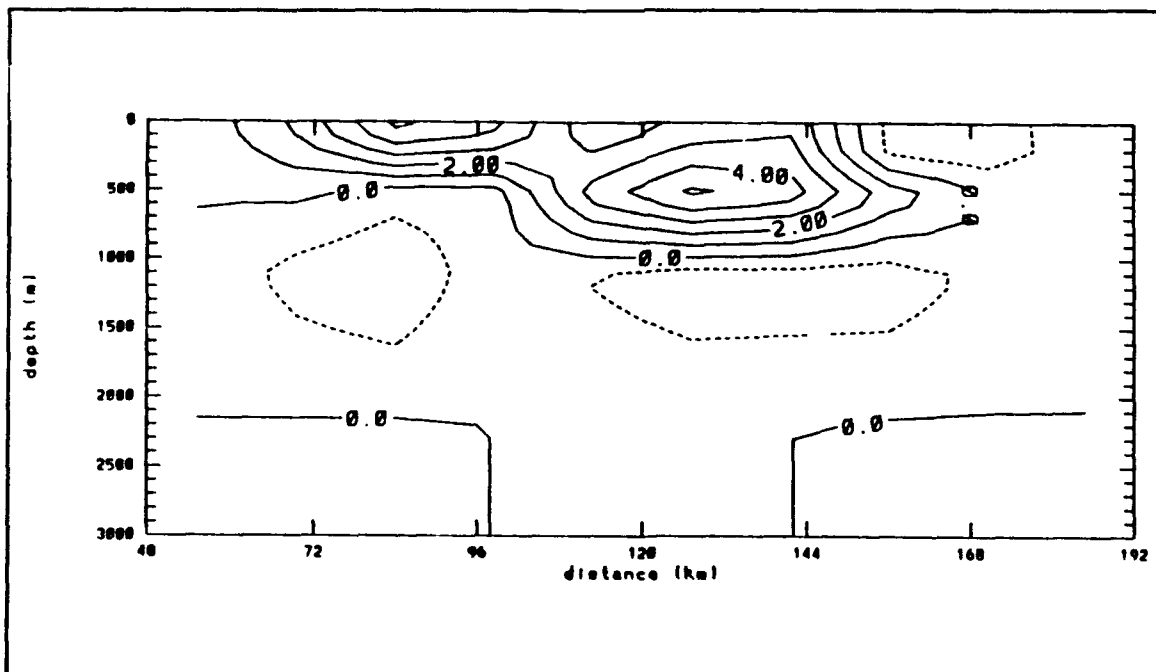


Figure 5. ESTIMATED  $\delta c$  FOR DAY 282 USING THE STATIC RAY APPROXIMATION. (contour interval in 1 m/s)

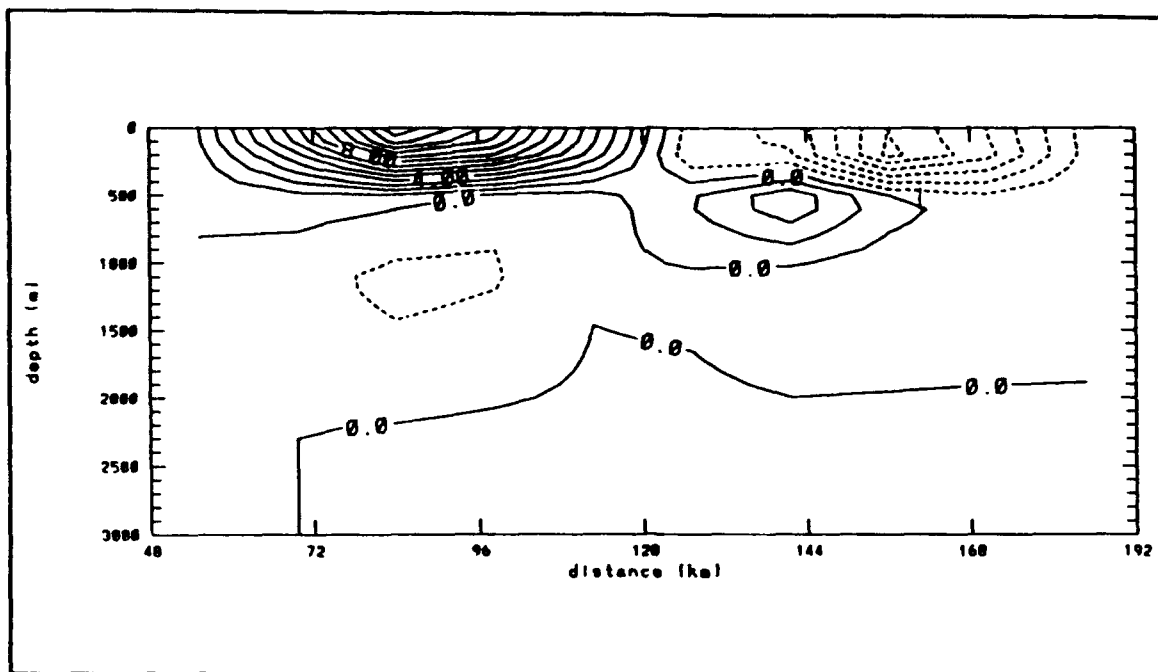


Figure 6. ESTIMATED  $\delta c$  FOR DAY 294 USING THE STATIC RAY APPROXIMATION. (contour interval is 1 m/s)

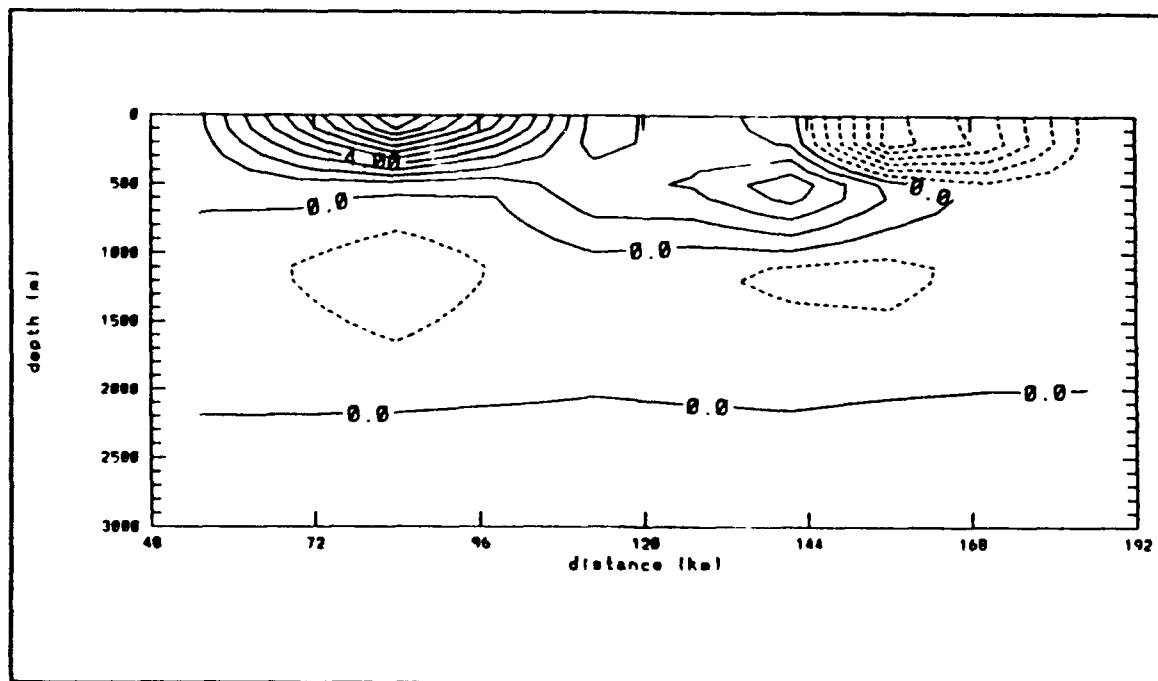


Figure 7. ESTIMATED  $\delta c$  FOR DAY 306 USING THE STATIC RAY APPROXIMATION. (contour interval is 1 m/s)

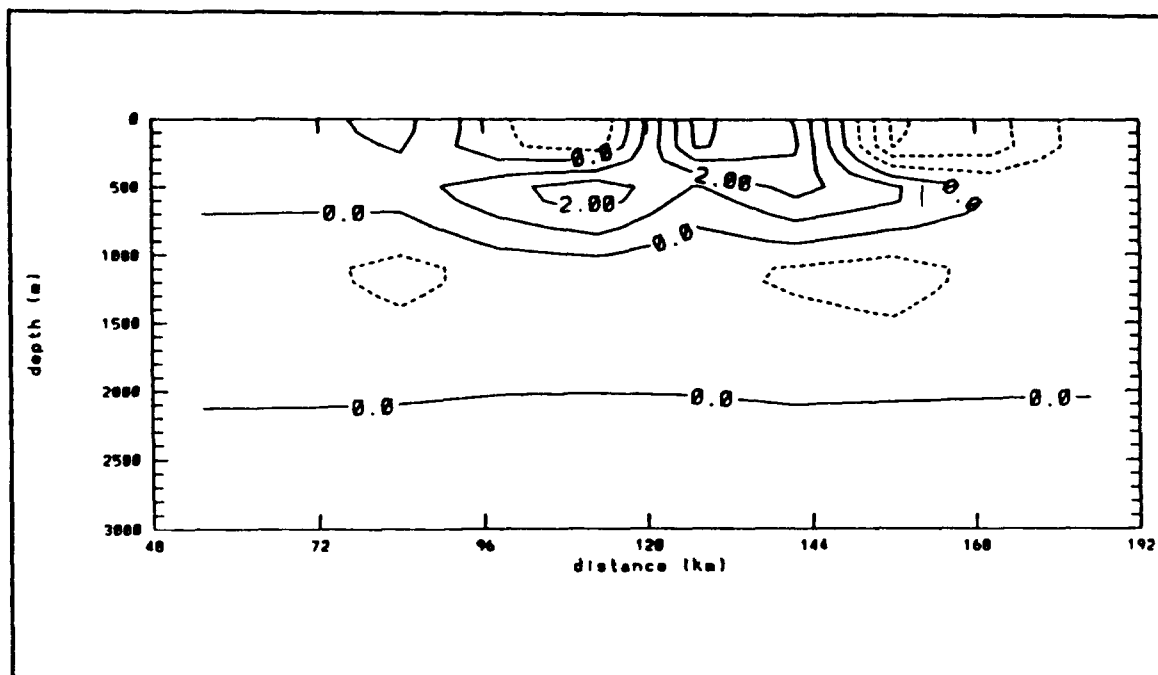


Figure 8. ESTIMATED  $\delta c$  FOR DAY 318 USING THE STATIC RAY APPROXIMATION. (contour interval is 1 m/s)

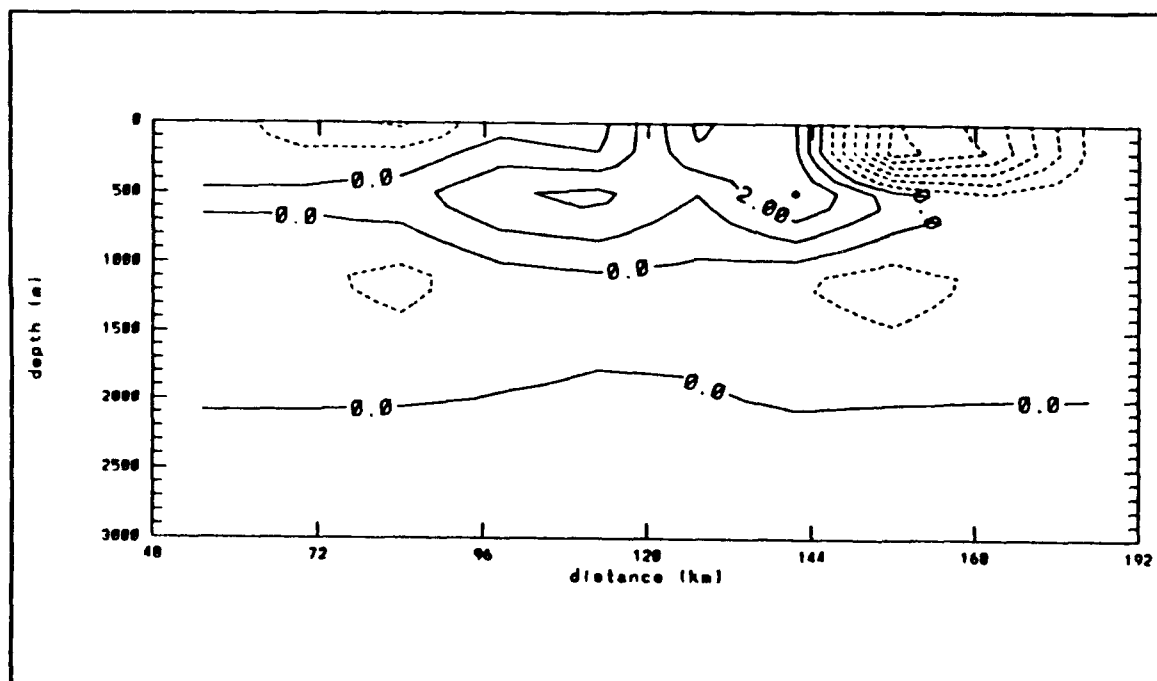


Figure 9. ESTIMATED  $\delta c$  FOR DAY 330 USING THE STATIC RAY APPROXIMATION. (contour interval is 1 m/s)



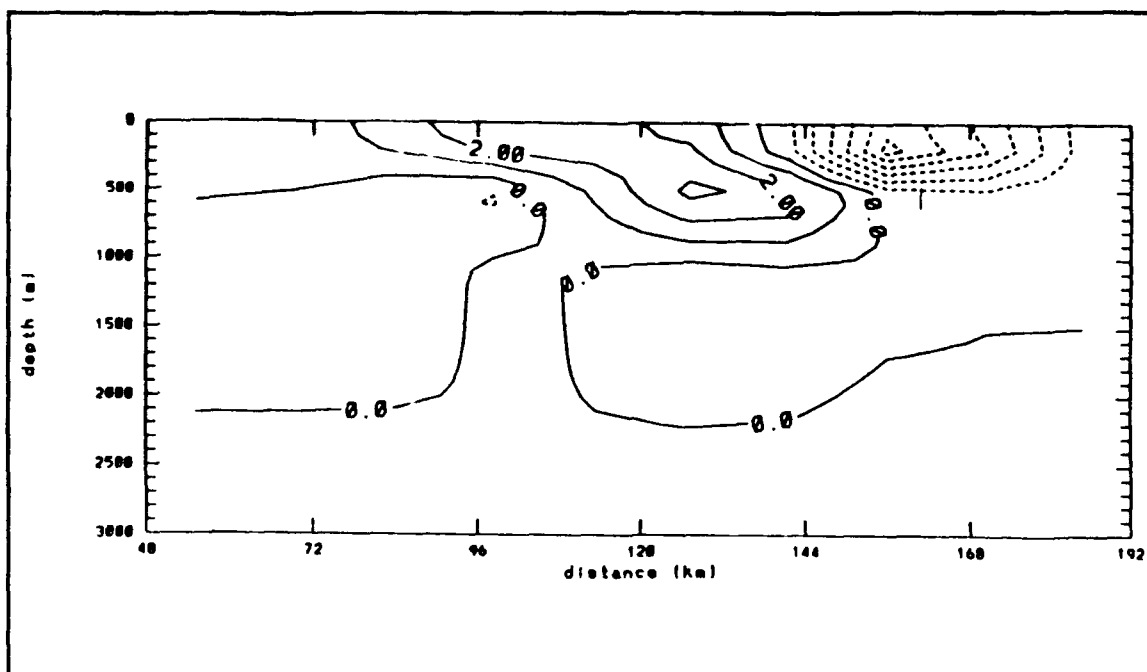


Figure 10. ESTIMATED  $\delta c$  FOR DAY 342 USING THE STATIC RAY APPROXIMATION. (contour interval is 1 m/s)

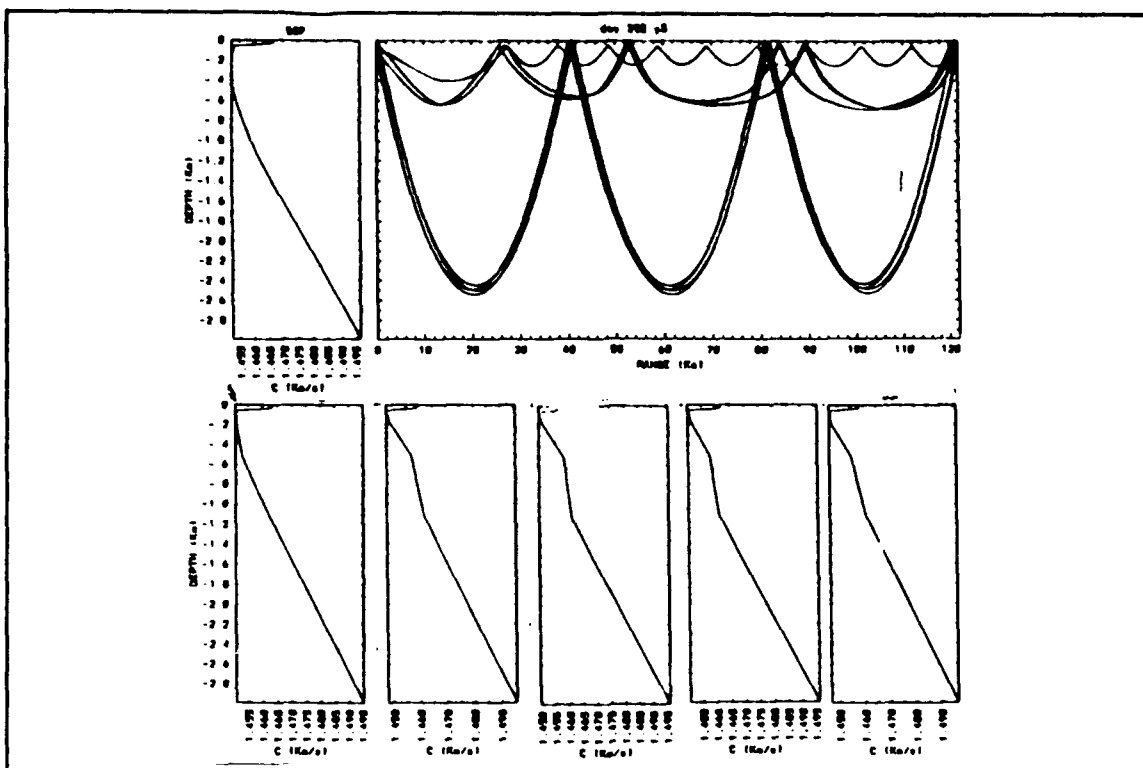
The  $\delta c$  maps estimated using the static ray approximation, shown in Figures 4-10, indicate an overall cooling of the ocean volume in the time period from day 270 through day 342. The upper 1000 m contains the largest amount of variability over this period. The ocean below 1500 m remains relatively stable.

There is a positive  $\delta c$  cell centered at approximately 84 km in the horizontal. This cell increases in intensity between days 270 and 294. The cell decreases in intensity after day 294. This decrease is continuous through day 342. A second positive  $\delta c$  cell is centered at approximately 140 km in the horizontal. This cell decreases in intensity between 270 and 294. Between days 294 and 342 the intensity remains

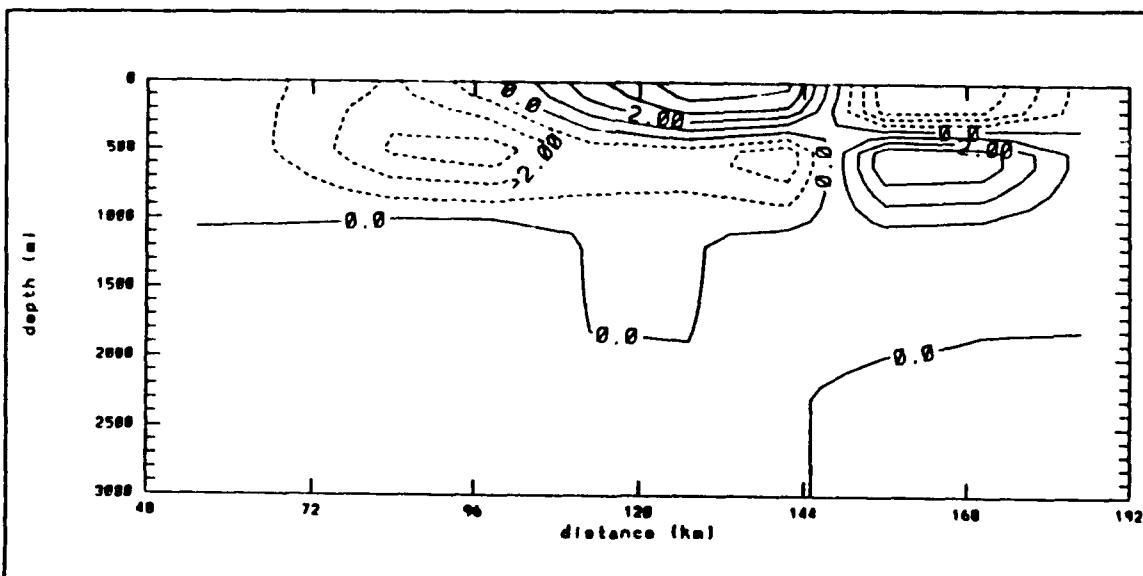
relatively constant and the horizontal area covered spreads out. There is a negative  $\delta c$  cell centered at approximately 168 km in the horizontal. The intensity of this cell appears to fluctuate throughout the entire study period. Finally, two negative  $\delta c$  cells are located at approximately 80 and 144 km in the horizontal and between 500 and 2000 m depths. The intensity of these cells remain constant from day 270 through day 342.

### C. INVERSION USING UPDATED RAY GEOMETRY

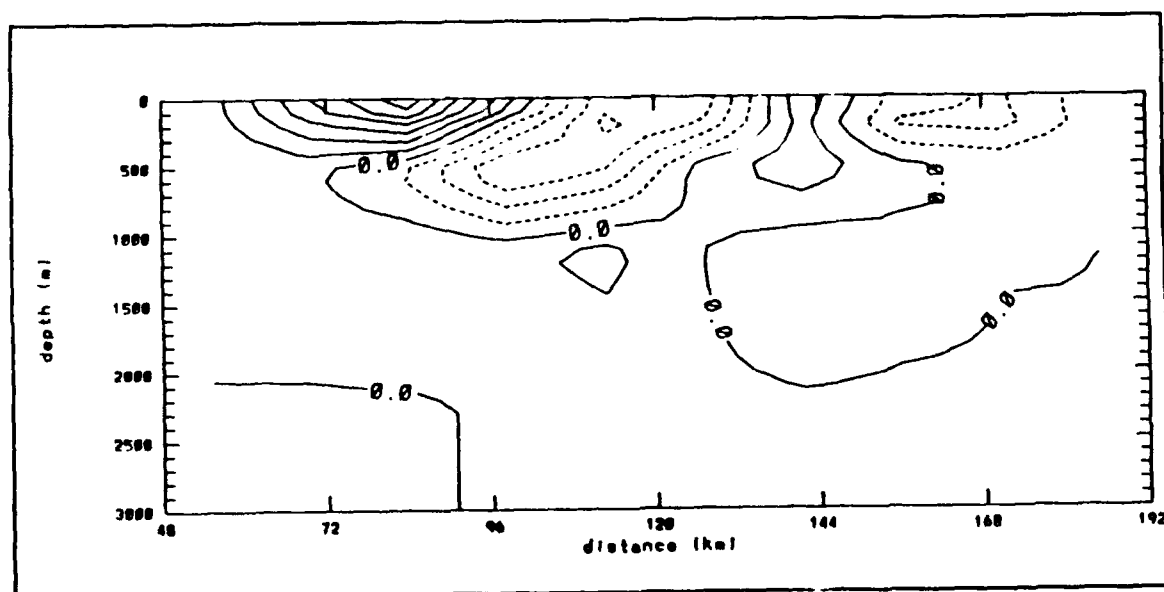
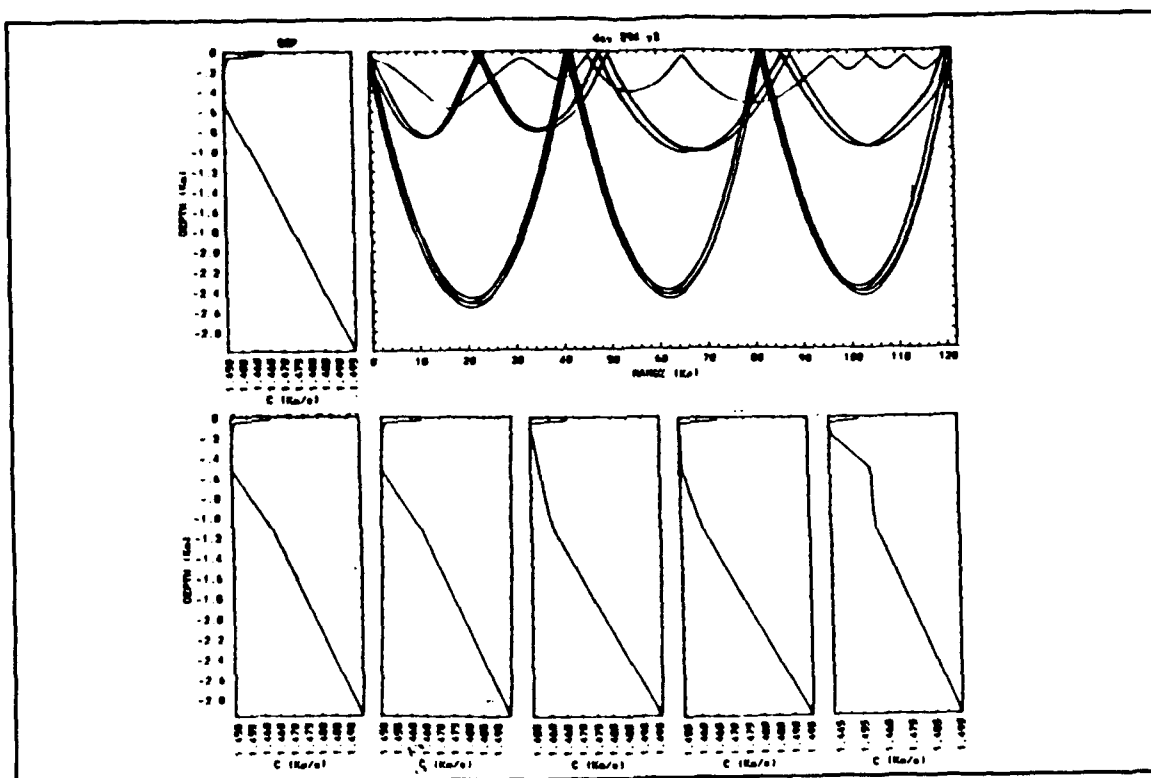
Inversions using updated ray geometry were conducted using the procedures previously outlined. Figure 3 shows the initial range independent background profile and the associated eigenrays used. The odd numbered figures between Figures 11-22 are the updated range dependent SVPs and the associated eigenrays calculated by MPP. The even numbered figures between Figures 11-22 are the estimated  $\delta c$  maps generated directly by the inversion code. These  $\delta c$  estimates were used to update the range dependent background profiles at the respective time steps. In order to facilitate the comparison with the static ray inversion results we show in Figures 23-28 the corresponding cumulative  $\delta c$  maps. The  $\delta c$  displayed in these latter maps are the changes with respect to the initial range independent background profile.



**Figure 11. BACKGROUND SVP AND UPDATED EIGENRAYS FOR DAY 282.** Starting in the upper left and moving counterclockwise; SVPs at 0 km, 24 km, 48 km, 72 km, 96 km, and 123 km.



**Figure 12. ESTIMATED  $\delta c$  USED TO UPDATE EIGENRAYS FOR DAY 282.** (contour interval is 1 m/s)



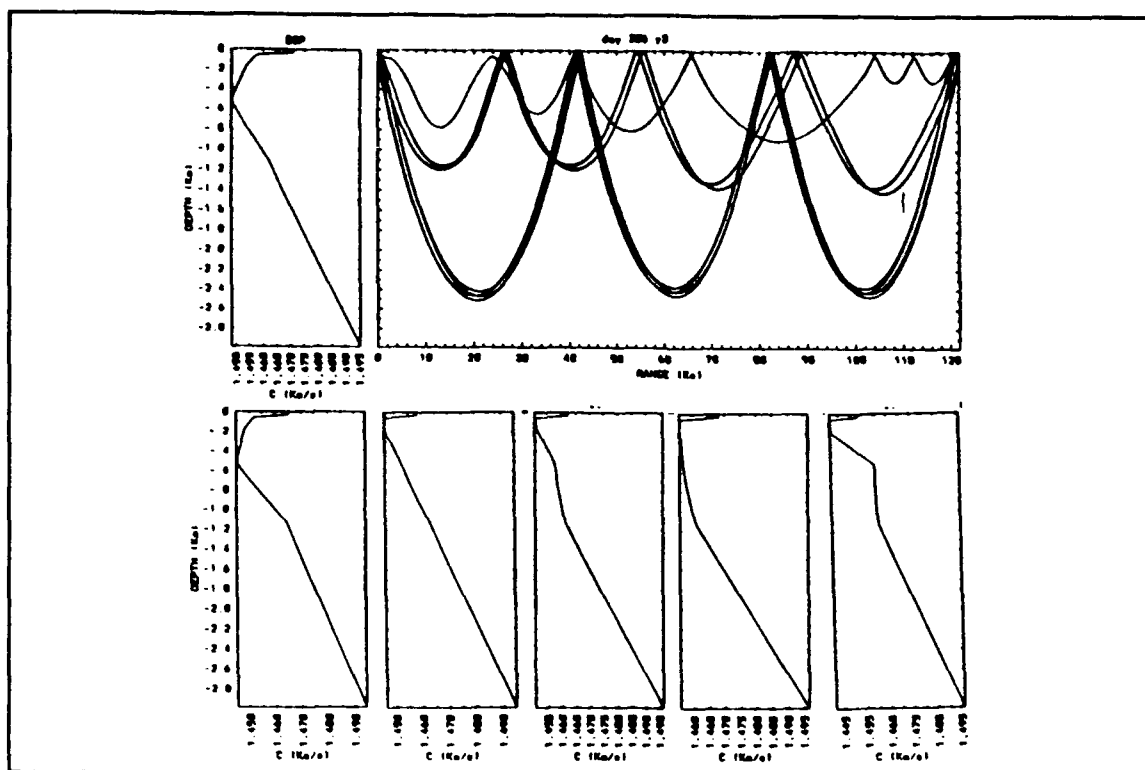


**Figure 15. BACKGROUND SVP AND UPDATED EIGENRAYs FOR DAY 306.** Starting in the upper left and moving counterclockwise; SVPs at 0 km, 24 km, 48 km, 72 km, 96 km, and 123 km.

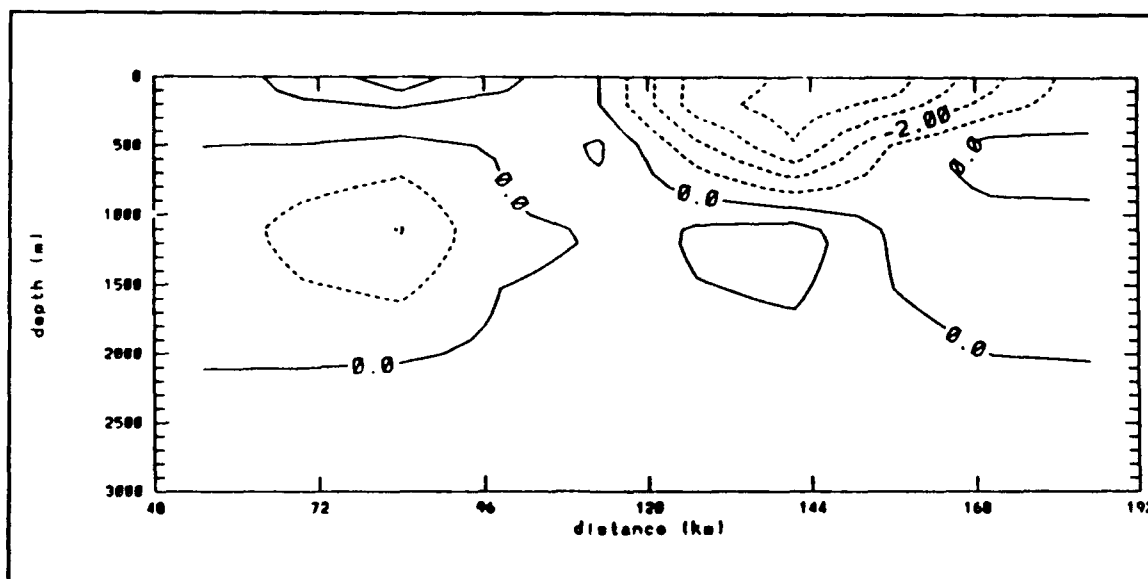


**Figure 16. ESTIMATED  $\delta c$  USED TO UPDATE EIGENRAYs FOR DAY 306.** (contour interval is 1 m/s)

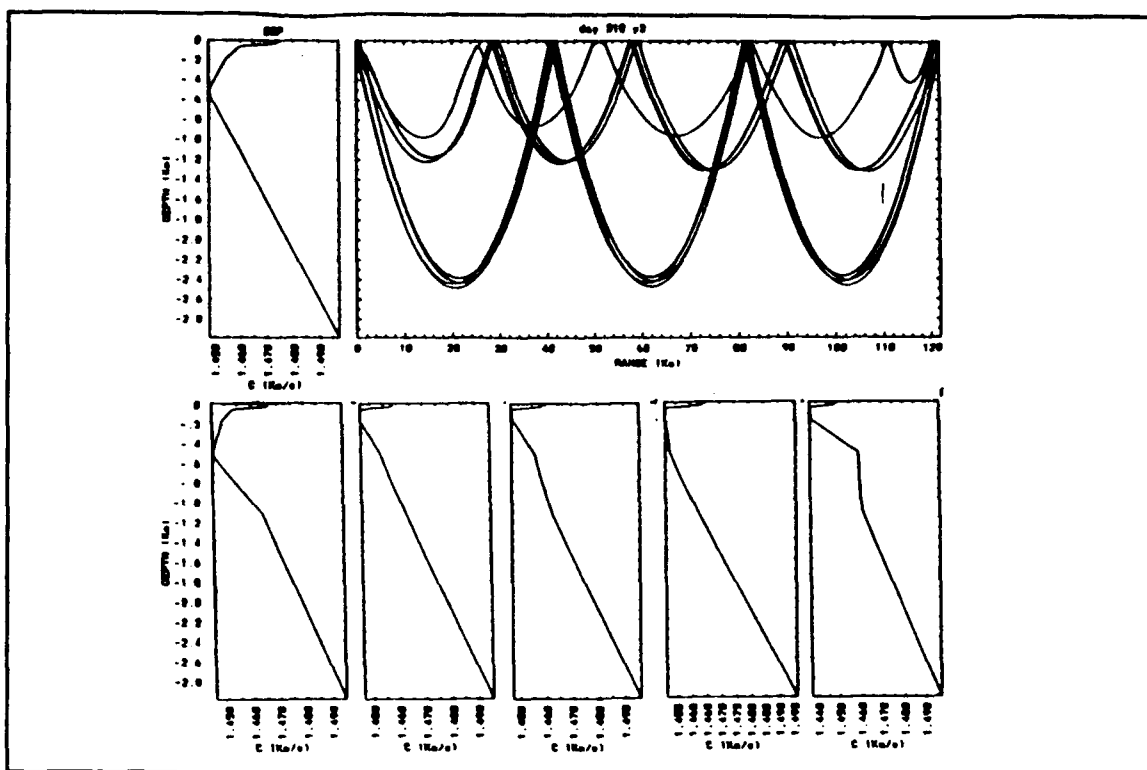


**Figure 17. BACKGROUND SVP AND UPDATED EIGENRAYS FOR DAY 318.** Starting in the upper left and moving counterclockwise; SVPs at 0 km, 24 km, 48 km, 72 km, 96 km, and 123 km.

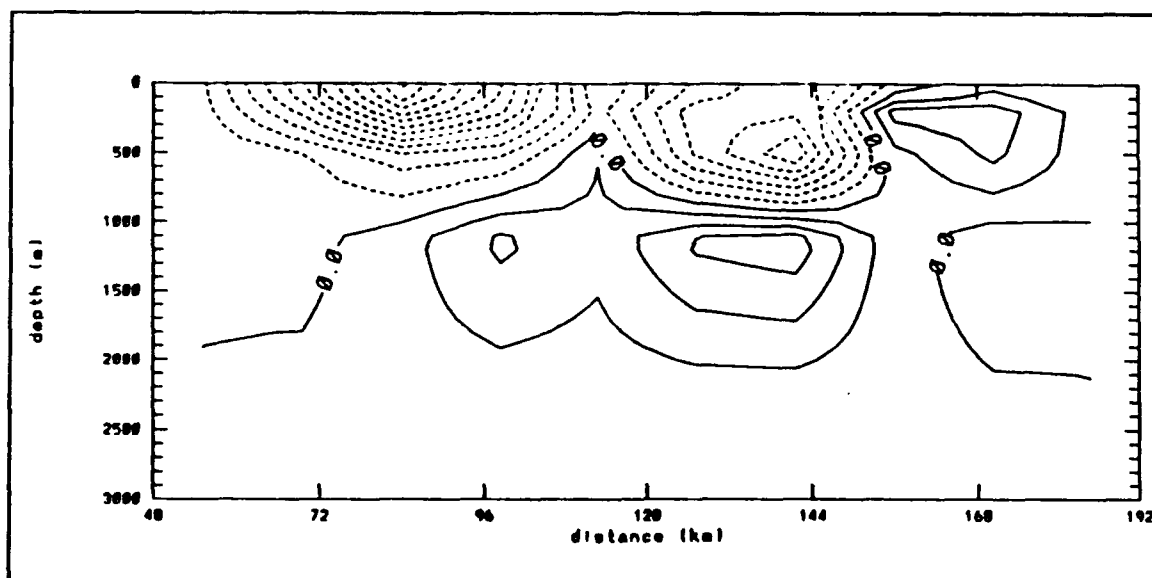


**Figure 18. ESTIMATED  $\delta c$  USED TO UPDATE EIGENRAYS FOR DAY 318.** (contour interval is 1 m/s)

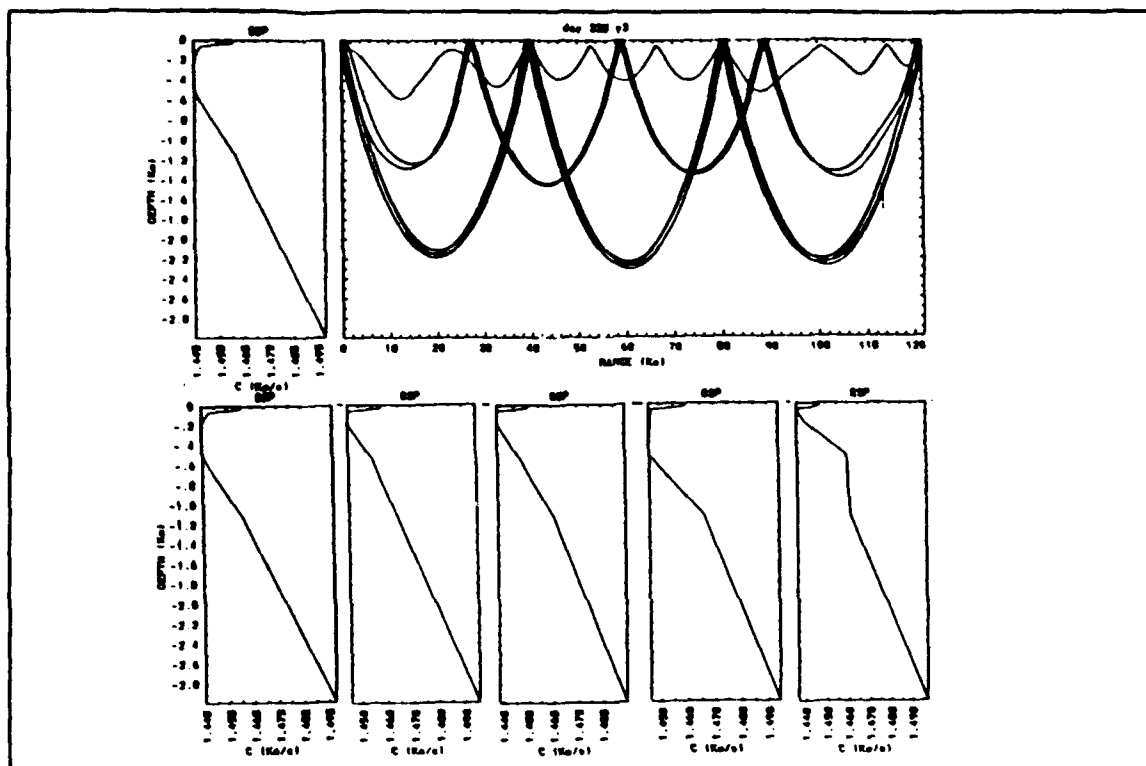


**Figure 19. BACKGROUND SVP AND UPDATED EIGENRAYs FOR DAY 330.** Starting in the upper left and moving counterclockwise; SVPs at 0 km, 24 km, 48 km, 72 km, 96 km, and 123 km.

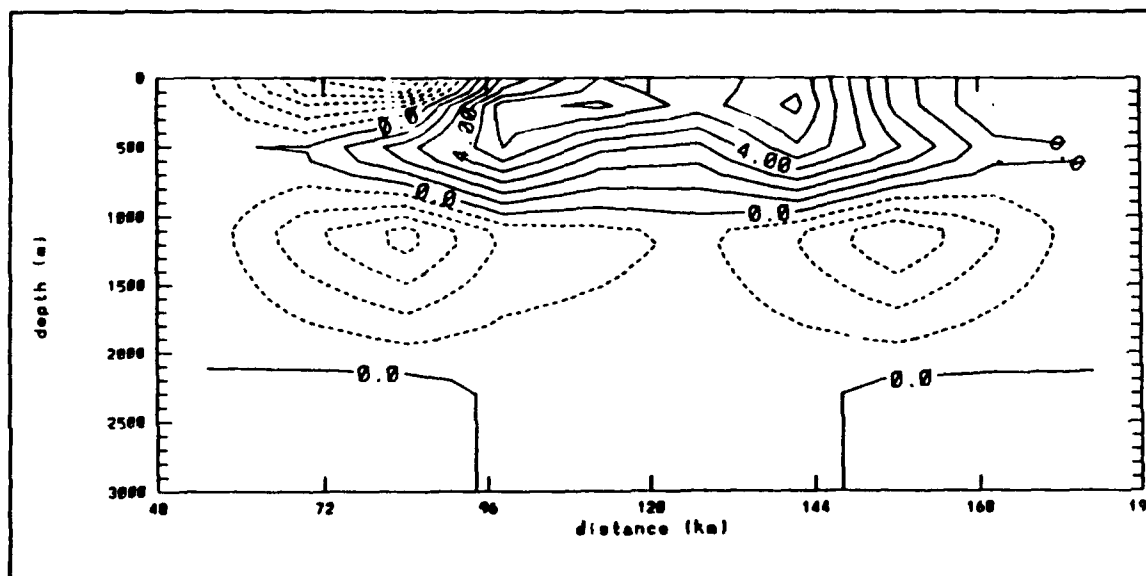


**Figure 20. ESTIMATED  $\delta c$  USED TO UPDATE EIGENRAYs FOR DAY 330.** (contour interval is 1 m/s)

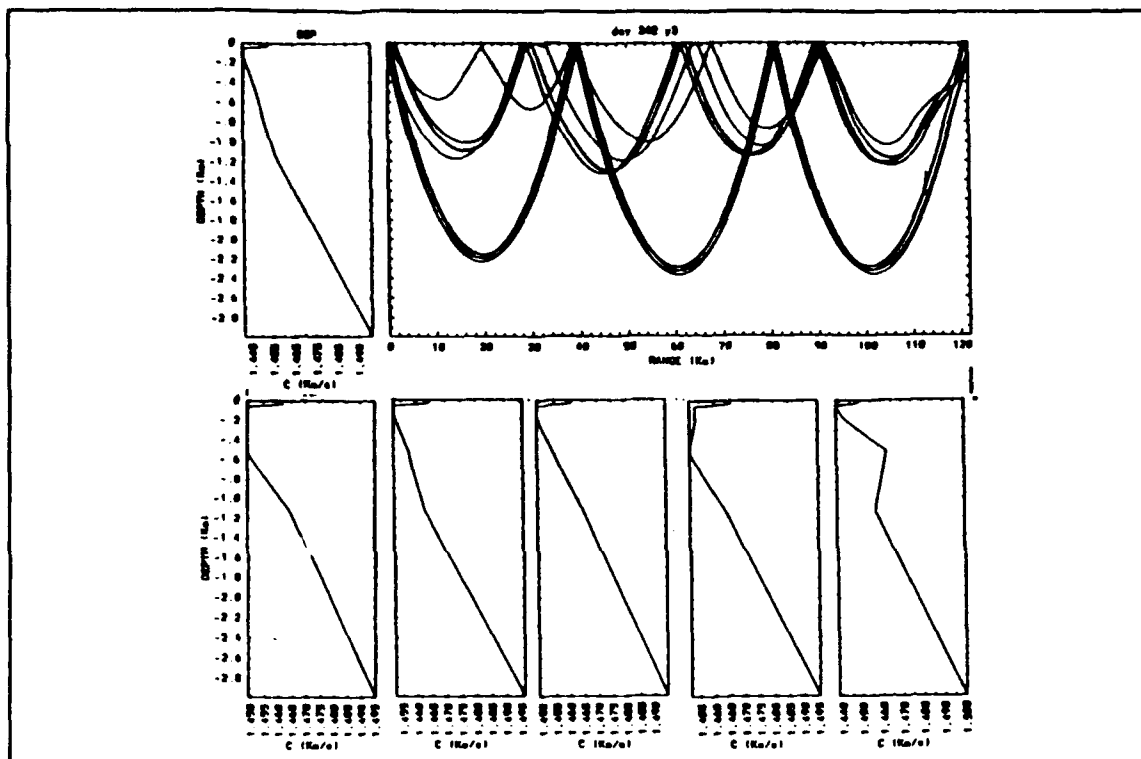


**Figure 21. BACKGROUND SVP AND UPDATED EIGENRAYs FOR DAY 342.** Starting in the upper left and moving counterclockwise; SVPs at 0 km, 24 km, 48 km, 72 km, 96 km, and 123 km.

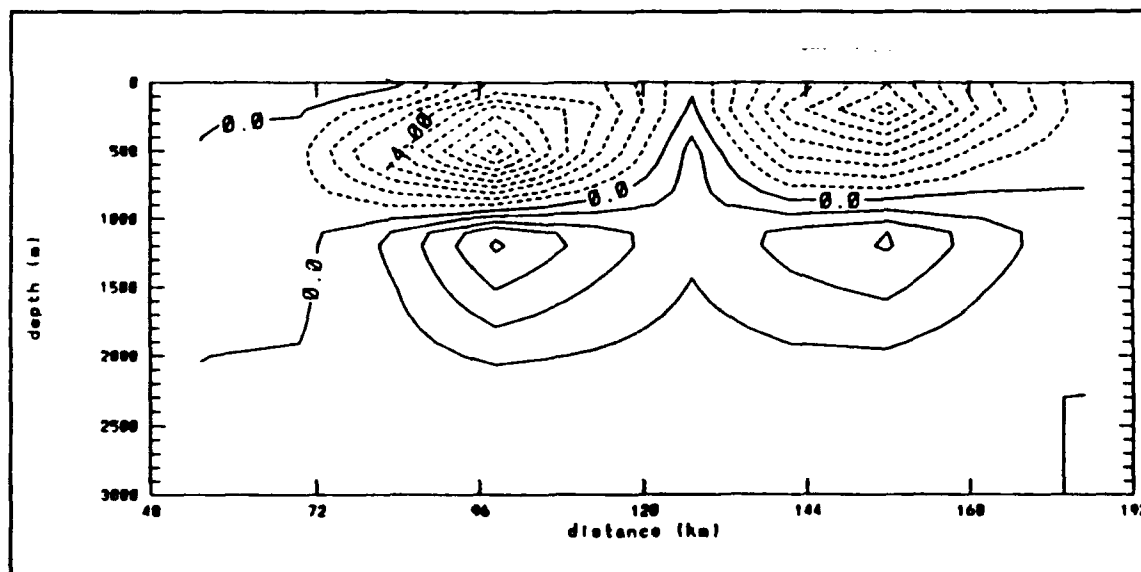


**Figure 22. ESTIMATED  $\epsilon c$  USED TO UPDATE EIGENRAYs FOR DAY 342.** (contour interval is 1 m/s)



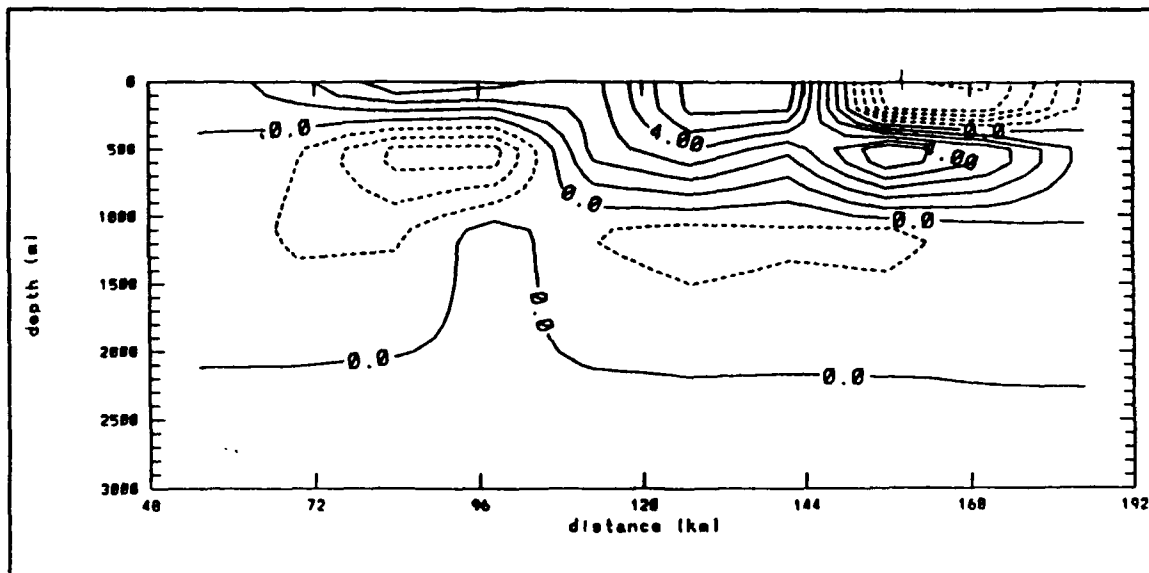


Figure 23. ESTIMATED CUMULATIVE  $\delta c$  FOR DAY 282 USING THE UPDATED RAY GEOMETRY. (contour interval is 1 m/s)

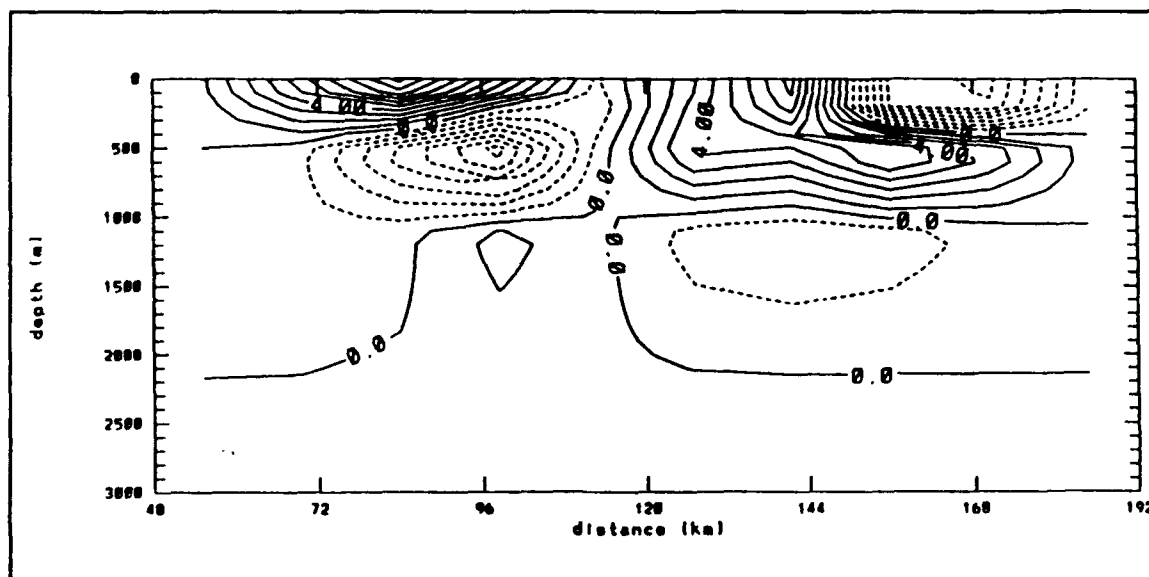
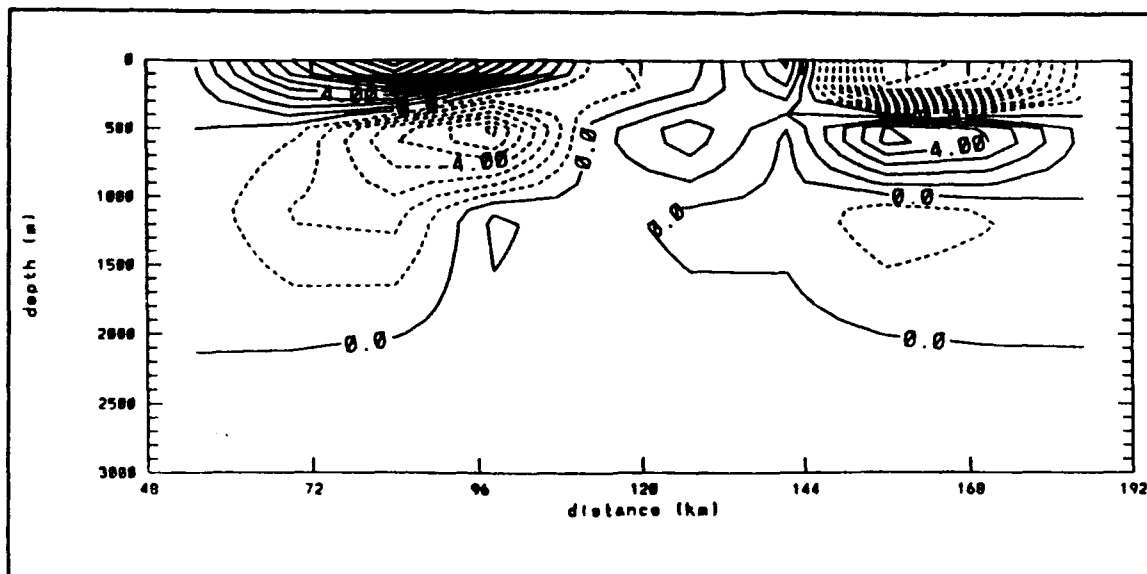
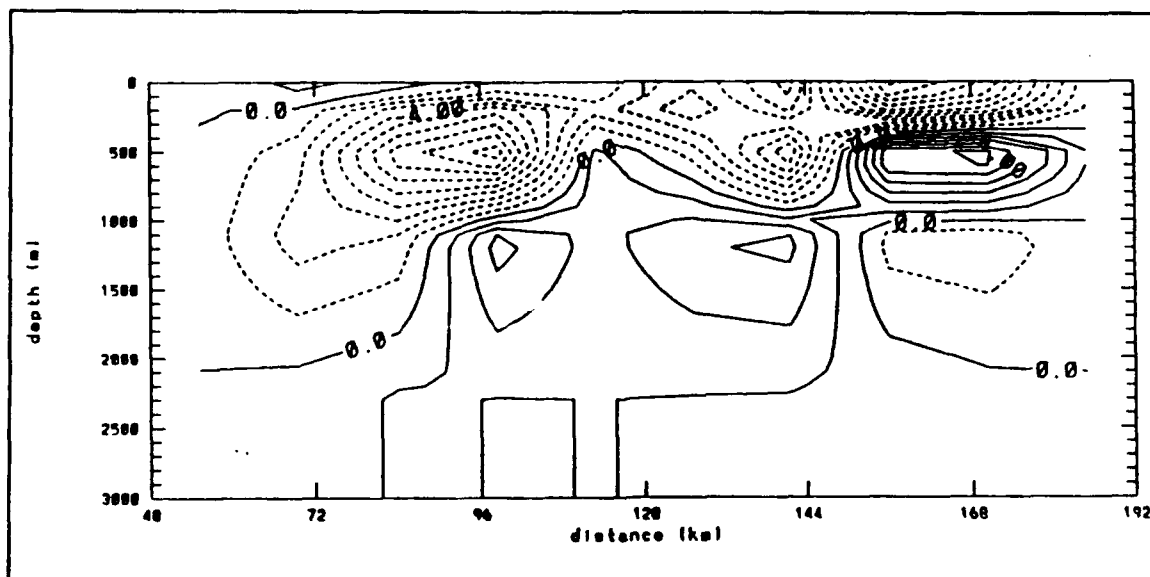


Figure 24. ESTIMATED CUMULATIVE  $\delta c$  FOR DAY 294 USING THE UPDATED RAY GEOMETRY. (contour interval is 1 m/s)



**Figure 25. ESTIMATED CUMULATIVE  $\delta c$  FOR DAY 306 USING THE UPDATED RAY GEOMETRY. (contour interval is 1 m/s)**



**Figure 26. ESTIMATED CUMULATIVE  $\delta c$  FOR DAY 318 USING THE UPDATED RAY GEOMETRY. (contour interval is 1 m/s)**

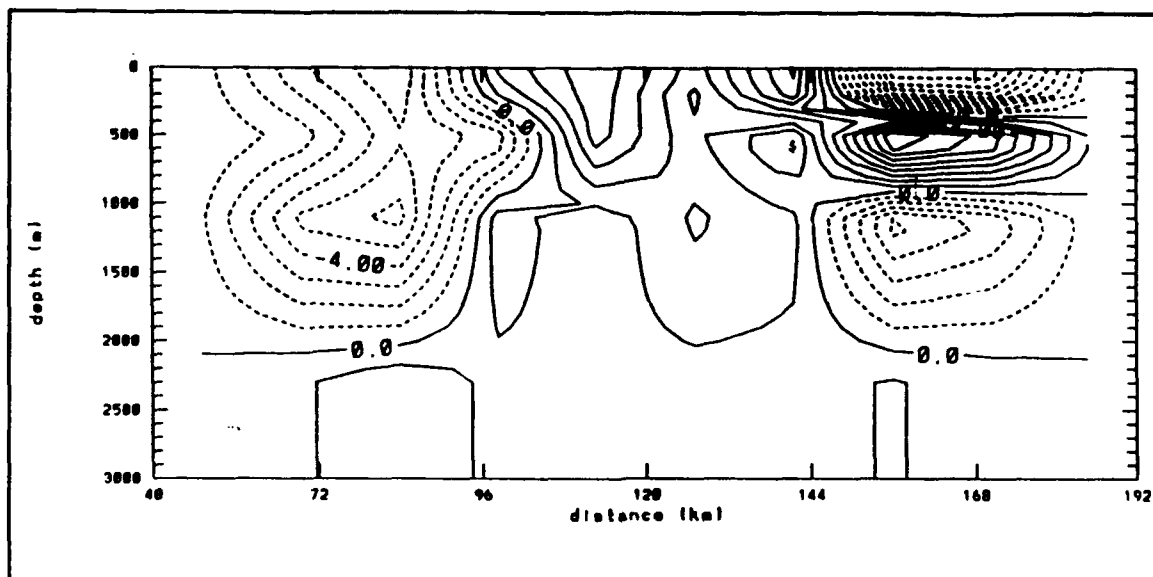


**Figure 27. ESTIMATED CUMULATIVE  $\delta c$  FOR DAY 330 USING THE UPDATED RAY GEOMETRY. (contour interval is 1 m/s)**

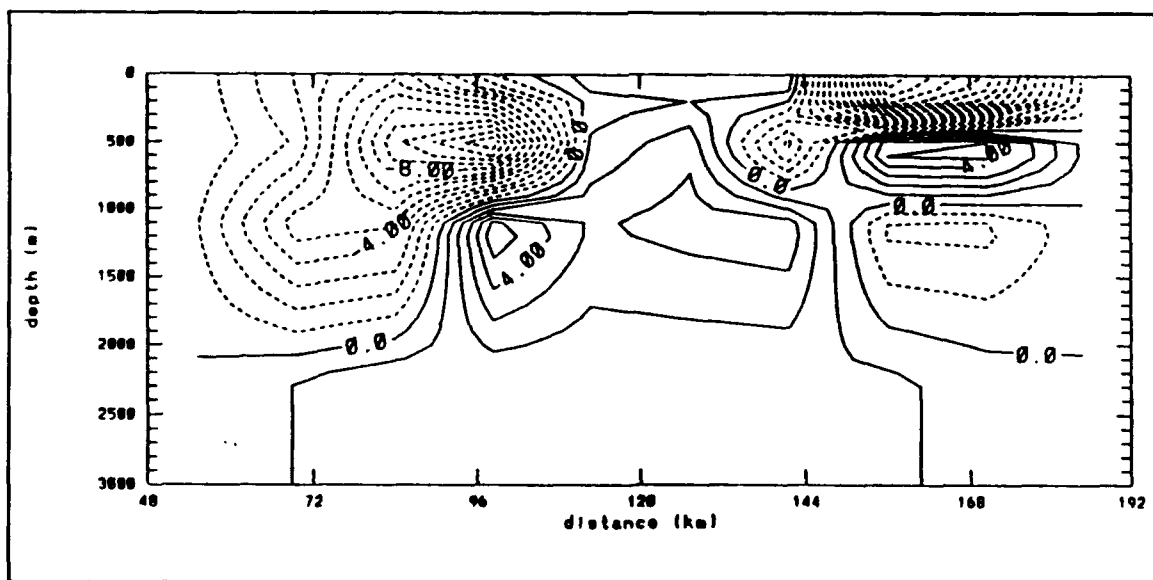


**Figure 28. ESTIMATED CUMULATIVE  $\delta c$  FOR DAY 342 USING THE UPDATED RAY GEOMETRY. (contour interval is 1 m/s)**

The  $\delta c$  maps, Figures 23-28, estimated using the updated ray geometry indicate that the largest amount of variability is now confined within the upper 2000 m of the ocean volume. The region below 2000 m has only slight changes.

Comparison of the  $\delta c$  maps generated using the updated ray geometry with those generated using the static ray approximation indicate that the two results are qualitatively similar. However, there are quantitative differences. The positive and negative  $\delta c$  cells correspond to approximately the same locations in the two inversions. Between days 270 and 306 the features appear to be approximately the same size in both the horizontal and the vertical directions. However, the features appear to be stronger in the inversion using the updated ray geometry. Between days 306 and 342 the features appear to be both larger and stronger in the inversion using the updated ray geometry.

An analysis of the eigenrays indicate that the 13 degree ray bundle remains stable over the period considered in this study. These rays spend the least amount of time in the area of high variability. The 10 degree ray bundle appears to be more variable and the zero degree ray is the most variable one. The variability of the eigenrays appears to increase as the amount of time the ray spends in the upper portion of the ocean volume increases.

#### IV. CONCLUSIONS AND RECOMMENDATIONS

The MPP raytraces indicate the presence of an absolute range error between the source at Mooring 4 and the receiver at Mooring 5 of approximately +322 m. Accounting for the absolute position error is important in reducing the amount of error introduced into the inverse solution.

If fluctuations in the ray path were having negligible effects,  $\delta c$  estimates generated by the two methods (*i.e.*, static ray approximation and updated ray geometry) should be approximately the same. Although the two inverse solutions are qualitatively similar, significant quantitative differences exist in the  $\delta c$  estimate generated by the two inversion methods.

It was also noted that the eigenrays were sensitive to the strong near-surface sound speed variability. The effects on the eigenrays were more pronounced the longer a ray spent in the near surface layer.

My conclusion is that it is necessary to account for the variability of the acoustic multipaths in the inversion of the Greenland Sea tomography data. This can be accomplished by updating the background profiles and ray geometry after every transmission day. Doing this will provide more accurate maps of the Greenland Sea gyre circulation through a winter cooling season.

## REFERENCES

- Chiu, C. S. and Y. Desaubies, "A Planetary Wave Analysis Using the Acoustic and Conventional Arrays in the 1981 Ocean Tomography Experiment", *Journal of Physical Oceanography*, 17, 1270-1287, 1987.
- Chiu, C. S., J. F. Lynch, and O. M. Johannessen, "Tomographic Resolution of Mesoscale Eddies in the MIZ - A Preliminary Study", *Journal of Geophysical Research*, 92(C7), 6886-6902, 1987.
- Cornuelle, B. D., and Collaborators, "Tomographic Maps of the Ocean Mesoscale. Part 1: Pure Acoustics", *Journal of Physical Oceanography*, 15, 133-152, 1985.
- Greenland Sea Science Planning Group, *Greenland Sea Project - An International Plan of the Arctic Ocean Sciences Board*, 1986.
- Joseph, J. E., *Acoustic Tomography in the Greenland Sea*, Master's Thesis, Naval Postgraduate School, Monterey, California, June 1991.
- Liebelt, P. B., *An Introduction to Optimal Estimation*, Addison Wesley, Inc., 1967.
- Munk, W. and C. Wunsch, "Ocean Acoustic Tomography: A Scheme for Large Scale Monitoring", *Deep Sea Research, Part A*, 26, 123-162, 1979.
- Spofford, C. W., "The Bell Laboratories Multiple-Profile Ray Tracing Programs," Bell Telephone Laboratories, 1973.

# INITIAL DISTRIBUTION LIST

- |   |   |
|---|---|
| 1. Defense Technical Information Center<br>Cameron Station<br>Alexandria, VA 22304-6145   | 2 |
| 2. Library, Code 52<br>Naval Postgraduate School<br>Monterey, CA 93943-5002   | 2 |
| 3. Chairman(Code OC/Co)<br>Department of Oceanography<br>Naval Postgraduate School<br>Monterey, CA 93943-5000                                       | 1 |
| 4. Chairman(Code AW/Er)<br>ASW Academic Group<br>Naval Postgraduate School<br>Monterey, CA 93943-5000   | 1 |
| 5. Professor Ching-Sang Chiu(Code OC/Ci)<br>Department of Oceanography<br>Naval Postgraduate School<br>Monterey, CA 93943-5000                      | 3 |
| 6. LCDR Peter J. Rovero(Code OC/Rv)<br>Department of Oceanography<br>Naval Postgraduate School<br>Monterey, CA 93943-5000                           | 1 |
| 7. Professor James F. Lynch<br>Department of Applied Ocean Physics<br>and Engineering<br>Woods Hole Oceanographic Institute<br>Woods Hole, MA 02543 | 1 |
| 8. LT Gary E. English<br>Department Head Class 123<br>SWOSCOLCOM<br>Newport, RI 02841   | 3 |